Acta Biochim Biophys Sin 2023, 55(5): 809–817
https://doi.org/10.3724/abbs.2023074
Advance Access Publication Date: 30 May 2023
Original Article

Original Article

ING5 overexpression upregulates miR-34c-5p/Snail1 to inhibit EMT and invasion of lung cancer cells

Jiong Yang[1,†], Xinli Liu[2,†], Yang Sun[2,†], Xutao Zhang[3], Yong Zhao[4], Haihua Zhang[5], Qibing Mei[2], Jin Meng[1,*], Feng Zhang[2,*], and Tao Zhang[5,*]

[1]Medical Supplies Center of PLA General Hospital, Beijing 100853, China, [2]Key Laboratory of Gastrointestinal Pharmacology of Chinese Materia Medica of the State Administration of Traditional Chinese Medicine, Department of Pharmacology, School of Pharmacy, Air Force Medical University, Xi'an 710032, China, [3]Department of Clinical Aerospace Medicine, Air force Medical University, Xi'an 710032, China, [4]Laboratory Animal Center, Air Force Medical University, Xi'an 710032, China, and [5]Department of Thoracic Surgery, Tangdu Hospital, Air Force Medical University, Xi'an 710038, China

[†]These authors contributed equally to this work.

*Correspondence address. Tel: +86-10-66775321; E-mail: yzmengjin@163.com (J.M.) / Tel: +86-29-84717564; E-mail: zhangf037@163.com (F.Z.) / E-mail: zhangft@fmmu.edu.cn (T.Z.)

Received 18 September 2022 Accepted 9 January 2023

Abstract

ING5 belongs to the inhibitor of growth (ING) candidate tumor suppressor family, which is involved in multiple cellular functions, such as cell cycle regulation, apoptosis, and chromatin remodelling. Previously, we reported that ING5 overexpression inhibits EMT by regulating EMT-related molecules, including Snail1, at the mRNA and protein levels. However, the mechanisms remain unclear. In the current study, we identify that ING5 overexpression induces the upregulation of miR-34c-5p. The expression levels of both ING5 and miR-34c-5p in NSCLC tissues from the TCGA database are decreased compared with that in adjacent tissues. Higher expression levels of both ING5 and miR-34c-5p predict longer overall survival (OS). Snail1 is the target gene of miR-34c-5p, as predicted by an online database, which is further verified by a dual-luciferase reporter assay. The expression level of Snail1 in NSCLC cells is markedly reduced following miR-34c-5p overexpression, leading to the inactivation of the Snail1 downstream TGF-β/Smad3 signaling pathway. The TGF-β signaling-specific inhibitor LY2157299 reverses the enhanced EMT, proliferation, migration, and invasion abilities induced by the miR-34c-5p inhibitor. Furthermore, tail vein injection of miR-34c-5p agomir inhibits xenografted tumor metastasis. Overall, this study concludes that miR-34c-5p, induced by ING5 overexpression, is a tumor suppressor that targets Snail1 and mediates the inhibitory effects of ING5 on the EMT and invasion of NSCLC cells. These results provide a novel mechanism mediating the antitumor effects of ING5.

Key words inhibitor of growth protein 5 (ING5), miR-34c-5p, non-small cell lung cancer (NSCLC), invasion and metastasis, diagnostic and prognostic biomarkers

Introduction

Lung cancer is the leading cause of cancer mortality due to its early metastasis [1]. The metastatic cascade involves highly complicated processes, including epithelial-mesenchymal transition (EMT) as the very early step, where epithelial cells acquire a migratory and mesenchymal phenotype [2,3]. EMT can be induced by various cellular factors and signals, among which Snail1 plays an important role in the induction and regulation of EMT [4,5]. ING5 belongs to the inhibitor of growth (ING) candidate tumor suppressor family [6,7]. Previously, we reported that ING5 overexpression inhibits EMT and invasiveness of lung cancer cells by regulating EMT-related molecules, including inhibition of Snail1 at both the mRNA and protein levels [8]; however, the mechanisms remain unclear.

MicroRNAs (miRNAs), a group of small noncoding RNAs, can influence gene expression via posttranscriptional regulation of mRNA [9,10]. The roles of miRNA dysregulation in malignancies

have been widely studied. By small RNA sequencing in A549 cells overexpressing ING5 and negative control cells, we identified differential expression levels of miRNAs regulated by ING5 overexpression, among which miR-34c-5p was significantly upregulated by ING5.

In the current study, we explored the correlation between ING5 and miR-34c-5p and further investigated the role of miR-34c-5p in the antitumor effects of ING5. We propose that ING5 may suppress EMT and invasion of lung cancer cells by upregulating miR-34c-5p to inhibit the Snail1/TGF-β/Smad3 signaling pathway.

Materials and Methods

Cell culture and reagents

The human lung cancer cell lines A549 and H1299 were purchased from the National Infrastructure of Cell Line Resource (Shanghai, China) and identified by Procell (Wuhan, China) in May 2019 according to the cell STR identification standard established by the International Cell Line Authentication Committee (ICLAC). Both A549 and H1299 cells were cultured in Dulbecco's modified Eagle's medium (HyClone, Logan, USA) supplemented with 10% fetal bovine serum (HyClone), 10 mg/mL antibiotics (penicillin and streptomycin), and 2 mM L-glutamine at 37°C in a humidified atmosphere with 5% CO_2. The TGF-β/Smad3 signaling pathway-specific inhibitor LY2157299 was obtained from Selleck (Houston, USA), and its 20 mM dimethyl sulfoxide (DMSO) stock solution was used for further studies.

Transfection of miRNA

The miR-34c-5p mimic (AGGCAGUGUAGUUAGCUGAUUGC) and mimic negative control (NC, UUGUACUACACAAAAGUACUG) were chemically synthesized and purified by HPLC (GenePharma, Shanghai, China). A549 and H1299 cells were transfected with the miR-34c-5p mimic or NC mimic using lipofectamine™ 2000 Transfection Reagent (Invitrogen, Carlsbad, USA) according to the manufacturer's instructions. Detailed information is as follows. First, 5 μL of miR-34c-5p mimic, NC mimic, and lipofectamine™ 2000 was added to 100 μL of Opti-MEM medium and incubated at room temperature for 5 min. Then, the mixture of miR-34c-5p mimic and NC mimic with Opti-MEM medium was gently added to the mixture of lipofectamine™ 2000 with Opti-MEM medium and incubated at room temperature for 20 min. Finally, 200 μL of miR-34c-5p mimic or NC mimic transfection mixture was added to each well and incubated at 37°C in a humidified atmosphere with 5% CO_2. After 8 h of transfection, the DMEM complete medium was replaced, and the cells were cultured for 24 h.

Luciferase reporter assay

The target gene of miR-34c-5p was predicted by the miRWalk 2.0 (http://mirwalk.umm.uni-heidelberg.de/) and miRDB (http://www.mirdb.org/cgi-bin/search.cgi) databases and then verified by dual-luciferase reporter assays. The binding sites between miR-34c-5p and its target gene *Snail1* were predicted by the miRWalk and miRDB databases. Snail1 with mutant (Mut) or wild-type (WT) binding sites was cloned into the pmiR-RB-REPORT™ vector (Promega, Madison, USA). The A549 cells were seeded in triplicate into 6-well plates at a density of 1×10^6 cells/well. The cells were transfected with NC + Snail1-WT, miR-34c-5p mimic + Snail1-WT, NC + Snail1-Mut, or miR-34c-5p mimic + Snail1-Mut using lipofectamine TM 2000. The dual-luciferase assay was carried out after 48 h of transfection using the Dual-Luciferase Reporter Assay System (Promega) according to the manufacturer's instructions.

RNA isolation and quantitative real-time PCR (qRT-PCR)

Total RNA was extracted from tumor tissues and cells by using TRIzol Reagent (Invitrogen) according to the manufacturer's instructions. RNA concentration was measured with a micro-ultraviolet spectrophotometer (NanoPhotometer™; Implen, München, Germany), and 1 μg of total RNA was reverse transcribed into cDNA by using the HiScript® Q select RT SuperMix for qRT-PCR Kit (+ gDNA wiper) (Vazyme, Nanjing, China) at the following thermal conditions: 95°C for 10 min and 40 cycles at 95°C for 15 s and 60°C for 1 min. Then, the cDNA was amplified using the ChamQTM SYBR® qPCR Master Mix (Vazyme) on a CFX96 Touch™ Real-Time PCR machine (Bio-Rad, Hercules, USA). The relative mRNA level was calculated using the $2^{-\Delta\Delta Ct}$ method. The experiments were performed in triplicate. Data were normalized using the housekeeping gene glyceraldehyde-3-phosphate dehydrogenase (*GAPDH*) or *U6* as an internal control.

Western blot analysis

Cells were lysed using lysis buffer containing 150 mM NaCl, 1% NP40, 0.5% deoxycholic acid, 0.1% SDS, 50 mM Tris (pH 8.0), and a 1:25 protease inhibitor cocktail for total protein. The protein concentration of the lysates was detected by the Bradford protein assay system (BCA; Bio-Rad). Protein samples were subject to SDS-PAGE, and transferred onto PVDF membranes. Membranes were blocked and incubated with primary antibodies at 4°C overnight. Primary antibodies, including anti-NOTCH1, anti-LDHA1, anti-E-cadherin, anti-N-cadherin, anti-Snail1, anti-TGF-β, anti-Smad3, anti-p-Smad3 were from Abcam (Cambridge, UK), and anti-actin and anti-GAPDH were from Santa Cruz Biotech (Santa Cruz, USA), and were used at a 1:1000 dilution. Then, membranes were incubated with goat anti-rabbit/mouse IgG (H + L)-HRP (Santa Cruz Biotech) secondary antibody at room temperature for 2 h. The protein signals were visualized using chemiluminescence reagent (PerkinElmer, Waltham, USA) and detected with an enhanced chemiluminescence western blotting detection system (Amersham Bioscience, London, UK).

Cell proliferation assay

Cells were seeded in triplicate into 96-well plates at a density of 1×10^4 cells/well and cultured overnight. Cells were treated with 20 μL of 5 mg/mL MTT solution (Sigma-Aldrich, St Louis, USA) after 24 h, 48 h, 72 h, 96 h, and 120 h of culture. Then, 150 μL of DMSO was added to each well to terminate the reaction. The absorbance of each well in the plate was measured with an iMark Microplate Reader (Bio-Rad) at 490 nm.

Colony formation assay

Cells were seeded in triplicate into 6-well plates at a density of 3×10^2 cells/well and cultured for approximately 2 weeks. Cells were fixed with 4% paraformaldehyde and then stained with 1% crystal violet (Jiancheng, Nanjing, China). Cell colony formation was detected with a CK-2 inverted microscope (Olympus, Tokyo, Japan), and the colony number was counted with ImageJ software (NIH, Bethesda, USA).

Wound healing assay

Cells were seeded in triplicate into 6-well plates at a density of 5 ×

10^5 cells/well and cultured overnight. A wound area was carefully created using a sterile 200 μL pipette tip when the cell density reached approximately 90%, and then detached cells were removed by rinsing with PBS. Images of cells were captured (100× magnification) with a CK-2 inverted microscope (Olympus, Tokyo, Japan) at 0 h, 6 h, 12 h, and 24 h.

Transwell migration and invasion assays

For the migration assay, the cells were suspended in serum-free medium and seeded in triplicate into the inserts of 24-well plate chambers at a density of 5×10^4 cells/well. For the invasion assay, the same number of cells were seeded in triplicate into the inserts of 24-well plate chambers coated with Matrigel (BD Bioscience, Franklin Lakes, USA) according to the manufacturer's instructions. Then, 600 μL complete medium was added into the lower chamber as a chemoattractant. The cells were then incubated for 12 h for the migration assay and 16 h for the invasion assay. Noninvasive cells in the upper chamber were removed by wiping with a cotton swab, and the invasive cells were fixed with 4% paraformaldehyde and then stained with 1% crystal violet. Cells on the surface of the lower chamber were imaged under the CK-2 inverted microscope. The inserts were washed with 33% acetic acid. The absorption was read immediately at 570 nm with an iMark Microplate Reader.

Xenograft model

Animal experiments were conducted according to ARRIVE guidelines and protocols formulated by the Animal Care and Use Committee of Fourth Military Medical University. Male athymic nude mice (6 weeks old) were purchased from the Experimental Animal Center of Fourth Military Medical University. For the intravenous mouse model, mice were randomly divided into 4 groups ($n = 5$) and injected with 5×10^6 A549 shControl cells or A549 shING5 cells through tail vein injection. Treatment was initiated on the day after injection. The dose of miR-34c-5p agomir (AGGCAGUGUAGUUAGCUGAUUGC) and agomir NC (UUGUACUACACAAAAGUACUG) (GenePharma, Shanghai, China) during treatment was 20 μg and administered daily for 14 days at 0.05–0.1 μg/kg/day through tail vein injection. Mice were euthanized and necropsied on day 40 after treatment, and lungs were inspected to assess the metastatic burden. The expression levels of ING5 and Snail1 in lung tumor tissues in nude mice were detected by immunohistochemical staining, and the expression level of miR-34c-5p was detected by qRT-PCR.

Statistical analysis

All statistical analyses were performed with SPSS 22.0 statistical software (IBM, Armonk, USA) and GraphPad Prism 7.0 software (GraphPad, San Diego, USA). Data were analysed by paired *t* test. Survival curves were estimated using the Kaplan-Meier method and compared using the log-rank test. Overall survival (OS) was determined from the date of surgery and histological diagnosis to the time of last contact or death due to any cause. All statistical analyses were two-tailed, and data were shown as the mean ± SD. $P < 0.05$ was considered statistically significant.

Results

ING5 overexpression upregulates miR-34c-5p and acts as a tumor suppressor in NSCLC

In this study, based on small RNA sequencing data, we screened and proved that hsa-miR-34c-5p (MIMAT0000686; Genechem, Shanghai, China) was upregulated by ING5 overexpression. We further confirmed the results by quantitative RT-PCR (qRT-PCR) (Figure 1A) with the expression level of miR-34c-5p 4.82-fold higher in ING5-overexpressing A549 cells than in A549 control cells.

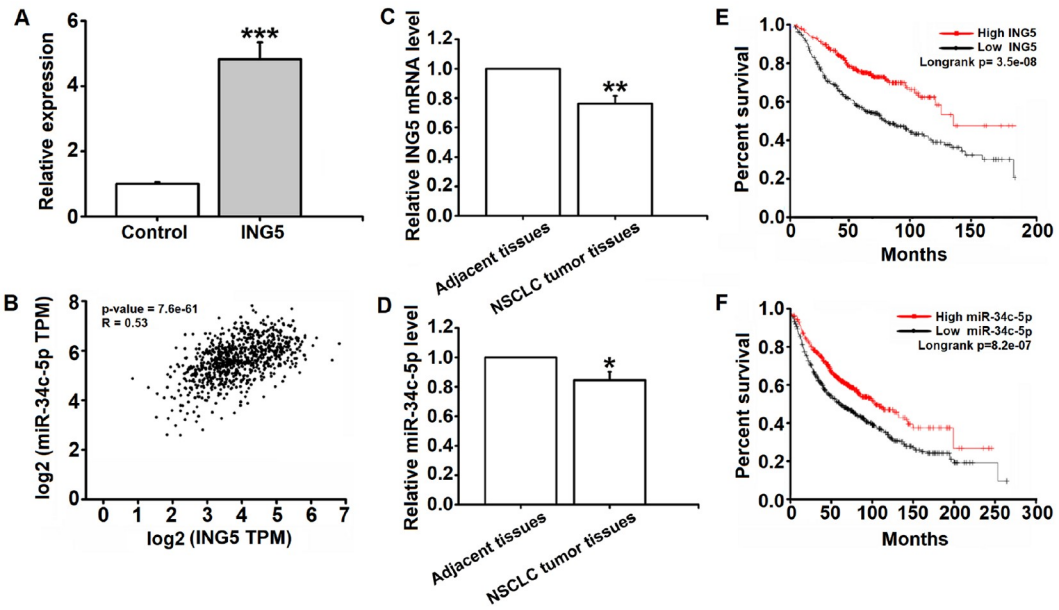

Figure 1. ING5 overexpression upregulates miR-34c-5p and acts as a tumor suppressor in NSCLC patients (A) The miR-34c-5p expression level in A549 control and A549-ING5 overexpression cells was measured by qRT-PCR. (B) Pearson correlation analysis of ING5 and miR-34c-5p in tumor tissues of patients with NSCLC in the TCGA database. (C,D) ING5 (C) and miR-34c-5p (D) expression levels in NSCLC tumor tissues in the TCGA database. (E,F) Kaplan-Meier analysis of the OS curves for NSCLC patients with high or low ING5 (E) or miR-34c (F) expression levels in the TCGA database. *U6* and *GAPDH* were used as reference genes. Data are shown as the mean ± SD, $n = 3$. Statistical analysis was performed using one-way ANOVA. *$P < 0.05$, **$P < 0.01$ and ***$P < 0.001$ vs NC group.

Consistently, the Pearson correlation analysis results showed that the expression levels of ING5 and miR-34c-5p in tumor tissues of NSCLC patients were positively correlated ($R = 0.53$, and $P = 7.6e{-}61$) (Figure 1B). We also analysed the expression levels of ING5 and miR-34c-5p in tumor tissues and adjacent tissues from patients with NSCLC in the TCGA database. The results showed that compared with adjacent tissues, both ING5 and miR-34c-5p expression levels in tumor tissues were decreased by 1.35-fold and 1.21-fold, respectively ($P < 0.05$) (Figure 1C,D). In addition, to determine whether ING5 or miR-34c-5p is associated with the overall survival (OS) of NSCLC patients, we stratified these patients into two different groups: patients with high ING5 or miR-34c-5p expression (relative expression level greater than median expression level) and patients with low ING5 or miR-34c-5p expression (relative expression level less than or equal to median expression level). The results showed that patients with low ING5 or miR-34c-5p expression had significantly lower OS than patients with high ING5 or miR-34c-5p expression (593 patients; log-rank $P = 0.0013$), as analysed by the log-rank test and Kaplan-Meier method (Figure 1E,F). Taken together, our results suggested that ING5 overexpression could upregulate miR-34c-5p, which might act as a tumor suppressor in patients with NSCLC.

Snail1 is a direct target gene of miR-34c-5p

To identify the target genes of miR-34c-5p, we performed a bioinformatics analysis using the miRDB (http://www.mirdb.org/index.html) database. As shown in Figure 2A. Snail1 was proven to be a potential target gene of miR-34c-5p. Then, we cotransfected wild-type (WT) Snail1 3′UTR dual-luciferase reporter plasmid, together with miR-34c-5p mimic or NC miRNA into HEK293T cells. As shown in Figure 2B, miR-34c-5p mimic significantly decreased the luciferase activity of Snail1-WT reporters. However, the miR-34c-5p mimic had little effect on luciferase activity when cotransfected with the mutated Snail1 3′UTR dual-luciferase

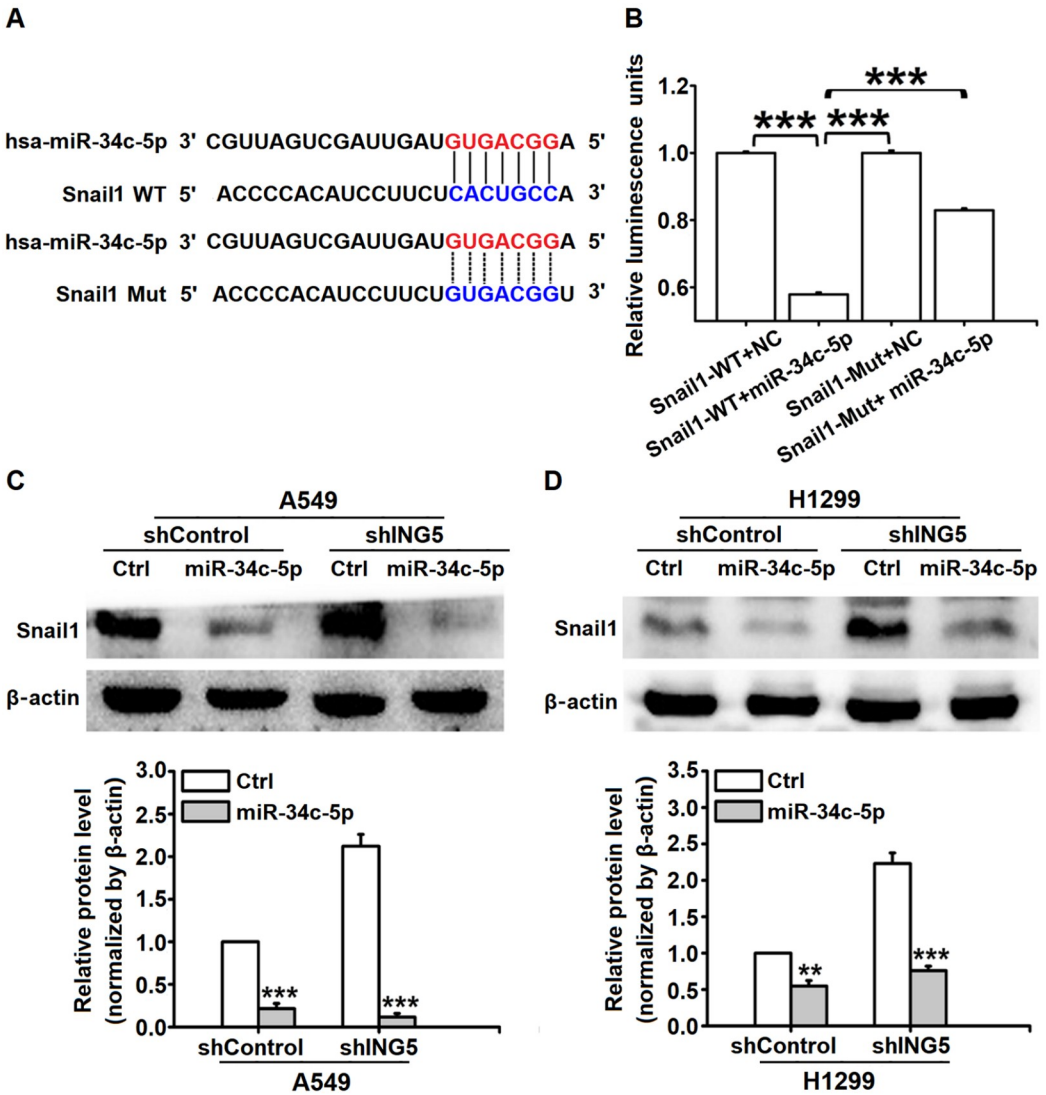

Figure 2. Snail1 is targeted and downregulated by miR-34c-5p (A) Prediction of the binding sites between miR-34c-5p and the *Snail* 1 3′UTR. (B) The dual-luciferase reporter assay. (C,D) Snail1 protein expression level after transfection with miR-34c-5p mimic in shControl and *ING5* knockdown A549 (C) and H1299 (D) cells detected by western blot analysis. β-Actin was used as a loading control. Data are shown as the mean ± SD, $n = 3$. Statistical analysis was performed using one-way or two-way ANOVA, followed by *post hoc* tests. $^{**}P < 0.01$ and $^{***}P < 0.001$ vs NC group.

reporter plasmid. Furthermore, western blot analysis results showed that the miR-34c-5p mimic dramatically decreased the protein levels of Snail1 in both A549 cells (Figure 2C) and H1299 cells (Figure 2D). These results confirmed that *Snail1* is a direct target of miR-34c-5p.

miR-34c-5p reverses *ING5* knockdown-induced EMT

To explore whether miR-34c-5p is involved in ING5-inhibited EMT, we transfected shControl A549 cells and *ING5*-knockdown A549 cells with miR-34c-5p mimic (Mimic) and mimic negative control (NC). Western blot analysis results revealed that the knockdown of *ING5* notably decreased the expression level of the epithelial marker E-cadherin, which was reversed by the miR-34c-5p mimic in A549 cells (Figure 3A) and H1299 cells (Figure 3B). In addition, *ING5* knockdown enhanced the expression levels of mesenchymal markers, including N-cadherin and EMT-related transcription factors Smad3, while they were downregulated after transfection with miR-34c-5p mimic ($P<0.05$). These results demonstrated that the inhibition of EMT was mediated by ING5/miR-34c-5p signaling.

miR-34c-5p is involved in the antiproliferative, antimigratory, and anti-invasive effects of ING5

To investigate whether miR-34c-5p mediates the anti-invasive effects of ING5, we treated *ING5*-knockdown A549 and H1299 cells and corresponding shControl cells with miR-34c-5p mimic and NC mimic, respectively. The results showed that *ING5* knockdown significantly increased the proliferation (Figure 4A,B), wound healing (Figure 4C,D), migration (Figure 4E,F), and invasion (Figure 4G,H) properties of A549 cells and H1299 cells, which were reversed by the miR-34c-5p mimic. These results demonstrated that enhanced expression of miR-34c-5p could inhibit lung cancer cell invasiveness and reverse the increased invasive abilities promoted by *ING5* knockdown.

miR-34c-5p inhibits the invasion and metastasis of NSCLC cells by blocking the TGF-β/Smad3 signaling pathway

Snail1 has been reported to activate the TGF-β2/Smad3 signaling pathway [11]. To elucidate whether miR-34c-5p functions by targeting the Snail1/TGF-β/Smad3 axis, we detected and found that both mRNA (Figure 5A) and protein (Figure 5B) levels of TGF-β and p-Smad3 were markedly decreased after transfection with miR-34c-5p mimic in NSCLC cells, which could be effectively reversed by its inhibitor. Next, the TGF-β-specific inhibitor LY2157299 was used to determine the roles of the TGF-β/Smad3 axis in miR-34c-5p-regulated EMT as well as the migration, invasion, and proliferation

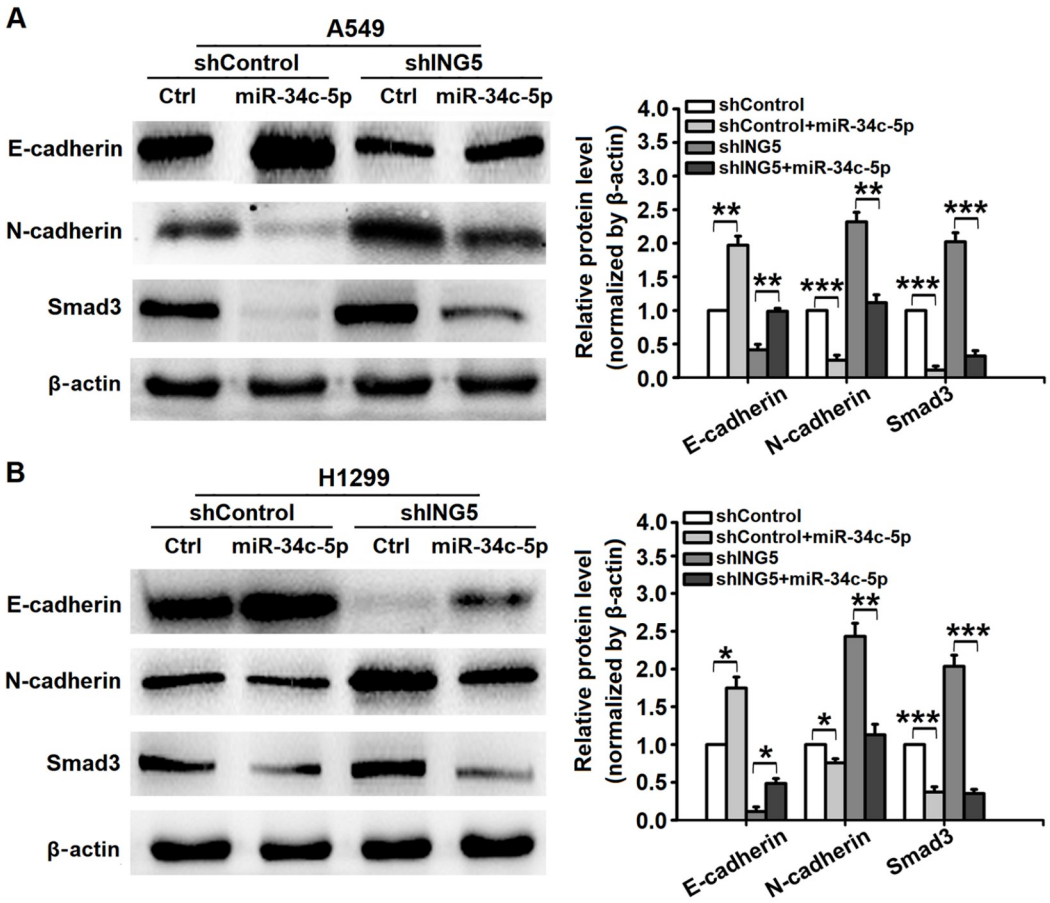

Figure 3. miR-34c-5p reverses *ING5* knockdown-induced EMT (A,B) Effect of miR-34c-5p on the protein expression levels of epithelial marker E-cadherin, mesenchymal marker N-cadherin, and EMT-related transcription factors Smad3 in *ING5*-knockdown A549 (A) and H1299 (B) cells compared with corresponding shControl A549 and H1299 cells detected by western blot analysis. β-Actin was used as a loading control. Data are shown as the mean ± SD, $n=3$. Statistical analysis was performed using one-way or two-way ANOVA, followed by *post hoc* tests. *$P<0.05$, **$P<0.01$ and ***$P<0.001$ vs NC group.

of NSCLC cells. A549 cells showed significantly enhanced colony formation (Figure 5C), migration (Figure 5D), invasion (Figure 5E), and proliferation (Figure 5F) abilities, as well as increased protein levels of TGF-β and p-Smad3 (Figure 5G) after transfection with miR-34c-5p inhibitor, whereas all these results were intensively abated by LY2157299 treatment. Taken together, these findings suggested that miR-34c-5p suppressed the invasiveness and EMT of NSCLC cells by targeting the Snail1/TGF-β/Smad3 signaling pathway.

miR-34c-5p prevents metastasis of *ING5*-knockdown lung cancer cells in nude mouse xenograft models

To investigate whether the miR-34c-5p signal is involved in *ING5* knockdown-promoted lung cancer invasiveness *in vivo*, we generated an intravenous nude mouse xenograft model by injecting A549 shControl or A549 shING5 cells through the tail veins of nude mice, which were then treated with miR-34c-5p agomir (Agomir) and agomir negative control (AC), respectively. Mice were sacrificed on day 40 after treatment, and the lungs were separated and inspected for tumor formation. All mice that were injected with A549 shControl and A549 shING5 cells developed multiple tumors in the bilateral lungs (Figure 6A). The mice treated with miR-34c-5p agomir had a significantly lower tumor index (Figure 6B) compared with the corresponding agomir negative control groups ($P < 0.05$). Furthermore, the results of qRT-PCR (Figure 6C) and immunohistochemical staining (IHC) (Figure 6D) demonstrated that both miR-

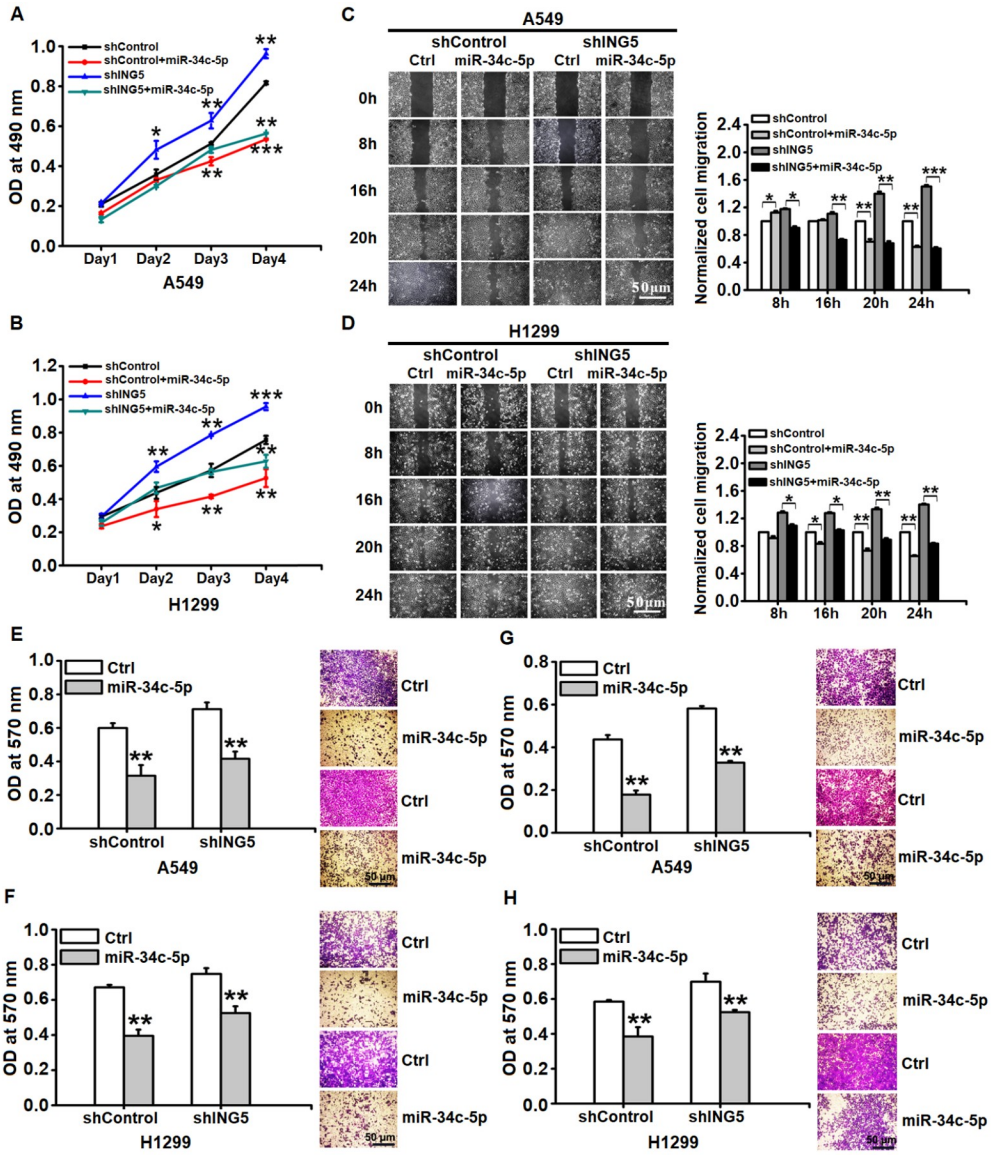

Figure 4. miR-34c-5p mediates the anti-proliferation, migration, and invasion effects of ING5 (A,B) Effect of miR-34c-5p on the cell viability of A549 shING5 (A) and H1299 shING5 (B) cells compared with the corresponding A549 shControl and H1299 shControl cells. (C,E) Effect of miR-34c-5p on the wound healing (C) and migration (E) of A549 shING5 cells compared with the corresponding A549 shControl cells. (D,F) Effect of miR-34c-5p on the wound healing (D) and migration (F) of H1299 shING5 cells compared with the corresponding H1299 shControl cells. (G,H) Effect of miR-34c-5p on the invasion of A549 shING5 (G) and H1299 shING5 (H) cells compared with the corresponding A549 shControl and H1299 shControl cells. Data are shown as the mean ± SD, $n = 3$. Statistical analysis was performed using one-way or two-way ANOVA, followed by *post hoc* tests. $^{*}P < 0.05$, $^{**}P < 0.01$ and $^{***}P < 0.001$ vs NC group.

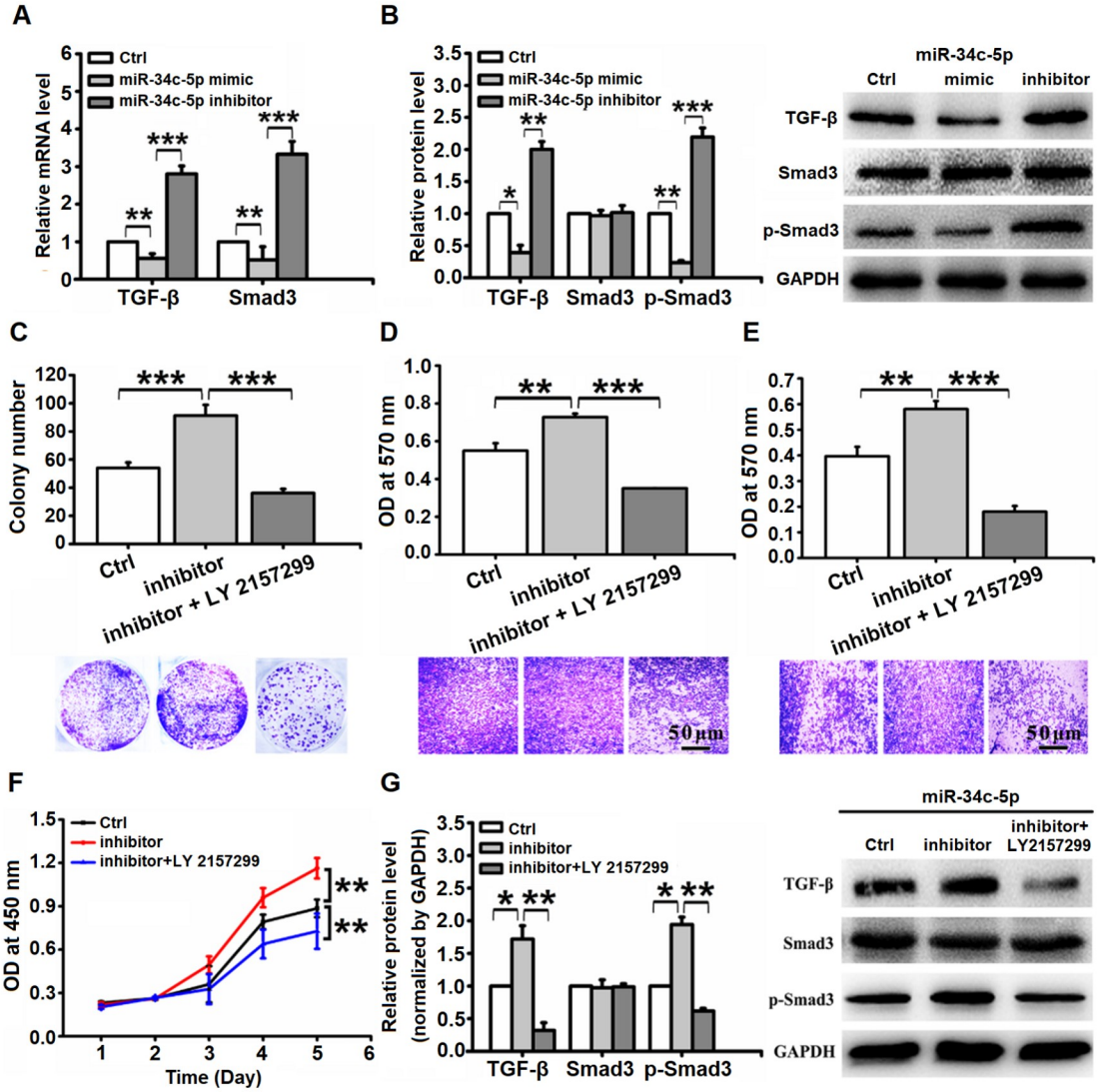

Figure 5. miR-34c-5p inhibits the proliferation, migration, invasion, and EMT of A549 cells in a manner dependent on the inactivation of the TGF-β/Smad3 signaling pathway (A,B) Both the mRNA (A) and protein expression (B) levels of TGF-β/Smad3 signaling pathway were detected in A549 cells after transfection with miR-34c-5p mimic or its specific inhibitor. (C–G) Effects of the TGF-β-specific inhibitor LY2157299 on colony formation (C), migration (D), invasion (E), proliferation (F), and protein expression levels of the TGF-β/Smad3 signaling pathway (G) in *miR-34c-5p*-knockdown A549 cells. GAPDH was used as a loading control. Data are shown as the mean ± SD, $n = 3$. Statistical analysis was performed using one-way or two-way ANOVA, followed by *post hoc* tests. *$P < 0.05$, **$P < 0.01$ and ***$P < 0.001$ vs NC group.

34c-5p and ING5 were significantly decreased, while Snail1 was increased in the lungs of the mice injected with A549 shING5 cells compared with those in the corresponding A549 shControl cells group ($P < 0.05$). Moreover, the mice treated with miR-34c-5p agomir exhibited increased expression levels of miR-34c-5p and ING5 and decreased expression level of Snail1 compared with the corresponding agomir negative control groups ($P < 0.05$). These results confirmed that miR-34c-5p could prevent the metastasis of *ING5*-knockdown lung cancer cells *in vivo*.

Discussion

Lung cancer remains the leading cause of cancer-related death worldwide because of its early metastasis [1,12]. Metastasis is a multistep event in which EMT is a critical process for cancer invasion and progression in the early stage [13–15]. EMT is the process by which epithelial cells lose their apical polarity, adopt a mesenchymal phenotype, and acquire migratory and invasive capacities [4]. EMT has been implicated in tumor progression and metastasis and is characterized by decreased epithelial marker E-cadherin and increased mesenchymal markers such as N-cadherin and Snail1 [5,16,17].

ING5 belongs to the inhibitor of growth (ING) candidate tumor suppressor family, which is involved in many cellular functions, including regulation of the cell cycle, apoptosis, DNA damage repair, and chromatin remodelling [18–21]. Our previous studies have revealed that ING5 inhibits the progression and invasion of lung cancer cells by regulating EMT-related molecules, including the inhibition of Snail1 at both the mRNA and protein levels [8,22,23]. However, the exact mechanisms are not fully understood.

miRNAs are small endogenous noncoding RNAs that act as

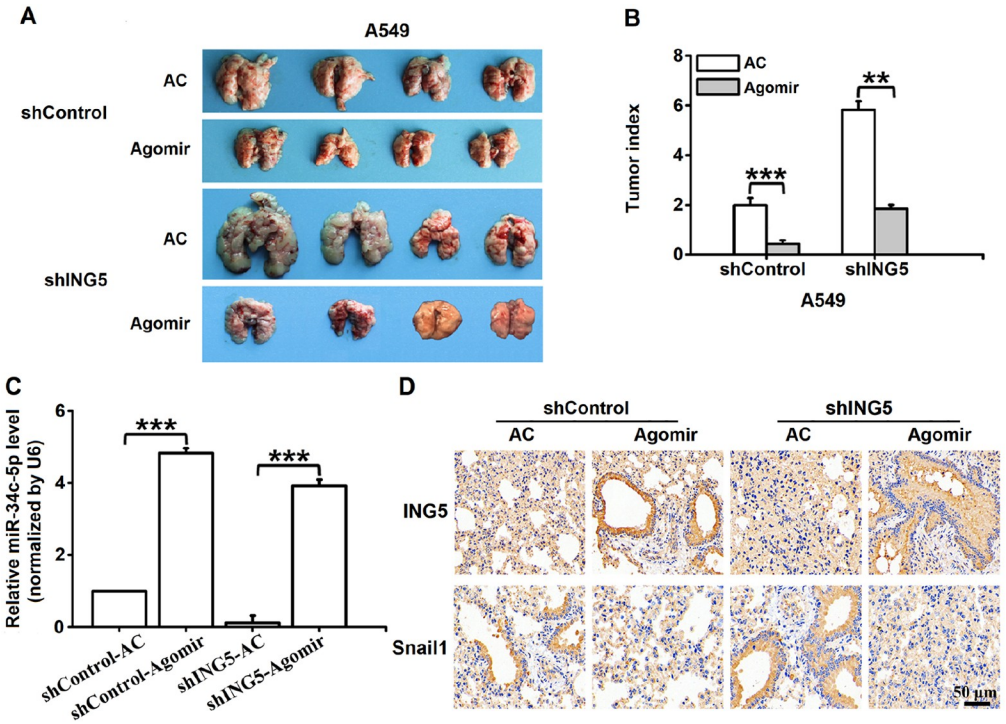

Figure 6. miR-34c-5p prevents metastasis of *ING5*-knockdown lung cancer cells in xenograft models (A) Mice were injected through the tail vein with 5×10^6 A549 shControl cells or A549 shING5 cells. On day 40 after tumour cell injection, the mice were sacrificed and photographed. Gross images of lungs showing lung-metastasized tumors in shControl and shING5 groups of mice with or without treatments. Representative images are shown. (B) Tumor index of mice from different groups. (C) Relative expression of miR-34c-5p in the lungs of mice in each group. *U6* was used as a reference gene. (D) Immunohistochemistry results of ING5 and Snail1 in the lungs of mice in each group. Data are shown as the mean ± SD, $n = 4$. Statistical analysis was performed using one-way ANOVA. $^{**}P < 0.01$ and $^{***}P < 0.001$ vs NC group.

oncogenes or tumor suppressors by regulating the expression levels of various genes associated with human cancers [24–27]. Dysregulation of miRNAs has been shown to be involved in cancer progression. In the current study, by small RNA sequencing, we identified differential expression levels of miRNAs regulated by ING5 overexpression, among which we focused on miR-34c-5p, whose expression level was significantly upregulated by ING5. Growing evidence has proposed that miR-34c-5p acts as a pivotal tumor suppressor in many cancer types [28–31]. miR-34c-5p was reported to target Notch1 and suppress the invasion and metastasis of cervical cancer cells [32]. miR-34c-5p also promotes the eradication of acute myeloid leukemia stem cells by targeting RAB27B to induce senescence and inhibit exosome shedding [33]. In this study, miR-34c-5p was proven to reverse *ING5* knockdown-induced EMT, migration, and invasion of lung cancer cells by downregulating its direct target Snail1 expression level.

Snail1, a zinc-finger transcription factor, plays a critical role in the regulation and induction of EMT by repressing E-cadherin transcription, thus leading to reduced cell adhesion and increased migratory capacity [34,35]. Snail1 high expression usually predicts poor prognosis in metastatic cancers [36,37]. Its involvement in the regulation of EMT and metastasis makes it a promising target for cancer treatment. Here, our results revealed that the expression level of Snail1 was increased in *ING5*-knockdown A549 and H1299 cells, which could be decreased after transfection with miR-34c-5p mimic. These results further confirmed the direct regulation of Snail1 by miR-34c-5p.

The transforming growth factor-β (TGF-β) signaling pathway is an indispensable inducer of EMT and tumor metastasis [38,39]. It has been reported that Snail1 overexpression could significantly activate the TGF-β2/Smad3 signaling pathway in breast cancer MCF-7 cells, while silencing of *Snail1* inhibited the transcription of *TGF-β2* and *Smad3*. Furthermore, enhanced TGF-β2 could promote both *Smad3* and *Snail1* transcription, which indicated a positive feedback regulatory loop between Snail1 and TGF-β2/Smad3 signals [11]. In this study, the TGF-β-specific inhibitor LY2157299 could effectively reverse the enhanced invasiveness and accelerated EMT process of lung cancer cells after silencing of miR-34c-5p by its specific inhibitor. These results further confirmed that miR-34c-5p functions as a tumor suppressor by targeting Snail1/TGF-β/Smad3 signaling.

In conclusion, we propose that miR-34c-5p is a tumor suppressor that targets Snail1 and mediates the inhibitory effects of ING5 on EMT and invasion in NSCLC. In particular, our study provides a novel mechanism underlying the antitumour effects of ING5.

Funding

This work was supported by the grants from the National Natural Science Foundation of China (Nos. 81802908 and 81672269).

Conflict of Interest

The authors declare that they have no conflict of interest.

References

1. Bray F, Ferlay J, Soerjomataram I, Siegel RL, Torre LA, Jemal A. Global cancer statistics 2018: GLOBOCAN estimates of incidence and mortality

worldwide for 36 cancers in 185 countries. *CA Cancer J Clin* 2018, 68: 394–424
2. Bronte G, Bravaccini S, Bronte E, Burgio MA, Rolfo C, Delmonte A, Crinò L. Epithelial-to-mesenchymal transition in the context of epidermal growth factor receptor inhibition in non-small-cell lung cancer. *Biol Rev* 2018, 93: 1735–1746
3. Mittal V. Epithelial mesenchymal transition in tumor metastasis. *Annu Rev Pathol* 2018, 13: 395–412
4. Bakir B, Chiarella AM, Pitarresi JR, Rustgi AK. EMT, MET, plasticity, and tumor metastasis. *Trends Cell Biol* 2020, 30: 764–776
5. Tseng JC, Lin CY, Su LC, Fu HH, Yang SD, Chuu CP. CAPE suppresses migration and invasion of prostate cancer cells via activation of non-canonical Wnt signaling. *Oncotarget* 2016, 7: 38010–38024
6. Dantas A, Al Shueili B, Yang Y, Nabbi A, Fink D, Riabowol K. Biological functions of the ING proteins. *Cancers* 2019, 11: 1817–1833
7. Zhang T, Meng J, Liu X, Zhang X, Peng X, Cheng Z, Zhang F. ING5 differentially regulates protein lysine acetylation and promotes p300 autoacetylation. *Oncotarget* 2018, 9: 1617–1629
8. Zhang F, Zhang X, Meng J, Zhao Y, Liu X, Liu Y, Wang Y, ***et al.*** ING5 inhibits cancer aggressiveness via preventing EMT and is a potential prognostic biomarker for lung cancer. *Oncotarget* 2015, 6: 16239–16252
9. Niu Y, Su M, Wu Y, Fu L, Kang K, Li Q, Li L, ***et al.*** Circulating plasma miRNAs as potential biomarkers of non–small cell lung cancer obtained by high-throughput real-time PCR profiling. *Cancer Epidemiol Biomarkers Prevention* 2019, 28: 327–336
10. Santarelli L, Gaetani S, Monaco F, Bracci M, Valentino M, Amati M, Rubini C, ***et al.*** Four-miRNA signature to identify Asbestos-related lung malignancies. *Cancer Epidemiol Biomarkers Prev* 2019, 28: 867–881
11. Lee DE, Jang EH, Bang C, Kim GL, Yoon SY, Lee DH, Koo J, ***et al.*** Bakuchiol, main component of root bark of Ulmus davidiana var. japonica, inhibits TGF-β-induced in vitro EMT and in vivo metastasis. *Arch Biochem Biophys* 2021, 709: 108969–108975
12. Duchemann B, Remon J, Naigeon M, Cassard L, Jouniaux JM, Boselli L, Grivel J, ***et al.*** Current and future biomarkers for outcomes with immunotherapy in non-small cell lung cancer. *Transl Lung Cancer Res* 2021, 10: 2937–2954
13. Hosseini K, Taubenberger A, Werner C, Fischer-Friedrich E. EMT-induced cell-mechanical changes enhance mitotic rounding strength. *Adv Sci* 2020, 7: 2001276
14. Vieugué P, Blanpain C. Recording EMT activity by lineage tracing during metastasis. *Dev Cell* 2020, 54: 567–569
15. Zhong C, Yang J, Lu Y, Xie H, Zhai S, Zhang C, Luo Z, ***et al.*** Achyranthes bidentata polysaccharide can safely prevent NSCLC metastasis via targeting EGFR and EMT. *Sig Transduct Target Ther* 2018, 5: 178–181
16. Li Y, Lv Z, Zhang S, Wang Z, He L, Tang M, Pu W, ***et al.*** Genetic fate mapping of transient cell fate reveals N-cadherin activity and function in tumor metastasis. *Dev Cell* 2020, 54: 593–607.e5
17. Sun L, Han T, Zhang X, Liu X, Li P, Shao M, Dong S, ***et al.*** PRRX1 isoform PRRX1A regulates the stemness phenotype and epithelial-mesenchymal transition (EMT) of cancer stem-like cells (CSCs) derived from non-small cell lung cancer (NSCLC). *Transl Lung Cancer Res* 2020, 9: 731–744
18. Coles AH, Jones SN. The ING gene family in the regulation of cell growth and tumorigenesis. *J Cell Physiol* 2009, 218: 45–57
19. Russell M, Berardi P, Gong W, Riabowol K. Grow-ING, Age-ING and Die-ING: ING proteins link cancer, senescence and apoptosis. *Exp Cell Res* 2006, 312: 951–961
20. Jafarnejad SM, Li G. Regulation of p53 by ING family members in suppression of tumor initiation and progression. *Cancer Metastasis Rev* 2012, 31: 55–73
21. Cui S, Liao X, Ye C, Yin X, Liu M, Hong Y, Yu M, ***et al.*** ING5 suppresses breast cancer progression and is regulated by miR-24. *Mol Cancer* 2017, 16: 89–100
22. Liu X, Meng J, Zhang X, Liang X, Zhang F, Zhao G, Zhang T. ING5 inhibits lung cancer invasion and epithelial–mesenchymal transition by inhibiting the WNT/β-catenin pathway. *Thoracic Cancer* 2019, 10: 848–855
23. Liu XL, Zhang XT, Meng J, Zhang HF, Zhao Y, Li C, Sun Y, ***et al.*** ING5 knockdown enhances migration and invasion of lung cancer cells by inducing EMT via EGFR/PI3K/Akt and IL-6/STAT3 signaling pathways. *Oncotarget* 2017, 8: 54265–54276
24. Li Q, Tong D, Guo C, Wu F, Li F, Wang X, Jiang Q, ***et al.*** MicroRNA-145 suppresses gastric cancer progression by targeting Hu-antigen R. *Am J Physiol Cell Physiol* 2019, 318: C605–C614
25. Khan P, Siddiqui JA, Lakshmanan I, Ganti AK, Salgia R, Jain M, Batra SK, ***et al.*** RNA-based therapies: a cog in the wheel of lung cancer defense. *Mol Cancer* 2021, 20: 54–65
26. Makarova J, Turchinovich A, Shkurnikov M, Tonevitsky A. Extracellular miRNAs and cell-cell communication: problems and prospects. *Trends Biochem Sci* 2021, 20: 54–77
27. Li Y, Yin Z, Fan J, Zhang S, Yang W. The roles of exosomal miRNAs and lncRNAs in lung diseases. *Sig Transduct Target Ther* 2019, 4: 47–58
28. Chiu SC, Chen KC, Hsia JY, Chuang CY, Wan CX, Wei TYW, Huang YRJ, ***et al.*** Overexpression of Aurora-A bypasses cytokinesis through phosphorylation of suppressed in lung cancer. *Am J Physiol Cell Physiol* 2019, 317: C600–C612
29. Huang W, Song W, Jiang Y, Chen L, Lu H. c-Myc-induced circ-NOTCH1 promotes aggressive phenotypes of nasopharyngeal carcinoma cells by regulating the miR-34c-5p/c-Myc axis. *Cell Biol Int* 2021, 20: 54–62
30. Abdel-Wahab AA, Effat H, Mahrous EA, Ali MA, Al-Shafie TA. A Licorice roots extract induces apoptosis and cell cycle arrest and improves metabolism via regulating miRNAs in liver cancer cells.*Nutr Cancer* 2020, 7: 1–12
31. Shen Y, Xu J, Pan X, Zhang Y, Weng Y, Zhou D, He S. LncRNA KCNQ1OT1 sponges miR-34c-5p to promote osteosarcoma growth via ALDOA enhanced aerobic glycolysis. *Cell Death Dis* 2020, 11: 278–286
32. Córdova-Rivas S, Fraire-Soto I, Mercado-Casas Torres A, Servín-González LS, Granados-López AJ. 5p and 3p strands of miR-34 family members have differential effects in cell proliferation, migration, and invasion in cervical cancer cells. *Int J Mol Sci* 2019, 20: 31–42
33. Peng D, Wang H, Li L, Ma X, Chen Y, Zhou H, Luo Y, ***et al.*** miR-34c-5p promotes eradication of acute myeloid leukemia stem cells by inducing senescence through selective RAB27B targeting to inhibit exosome shedding. *Leukemia* 2018, 32: 1180–1188
34. Espada J, Peinado H, Lopez-Serra L, Setién F, Lopez-Serra P, Portela A, Renart J, ***et al.*** Regulation of SNAIL1 and E-cadherin function by DNMT1 in a DNA methylation-independent context. *Nucleic Acids Res* 2011, 39: 9194–9205
35. Lambert IH, Nielsen D, Stürup S. Impact of the histone deacetylase inhibitor trichostatin A on active uptake, volume-sensitive release of taurine, and cell fate in human ovarian cancer cells. *Am J Physiol Cell Physiol* 2020, 318: C581–C597
36. Chen P, Kuang P, Wang L, Li W, Chen B, Liu Y, Wang H, ***et al.*** Mechanisms of drugs-resistance in small cell lung cancer: DNA-related, RNA-related, apoptosis-related, drug accumulation and metabolism procedure. *Transl Lung Cancer Res* 2020, 9: 768–786
37. Bartczak K, Białas AJ, Kotecki MJ, Górski P, Piotrowski WJ. More than a genetic code: epigenetics of lung fibrosis. *Mol Diagn Ther* 2020, 24: 665–681
38. Wang L, Tong X, Zhou Z, Wang S, Lei Z, Zhang T, Liu Z, ***et al.*** Circular RNA hsa_circ_0008305 (circPTK2) inhibits TGF-β-induced epithelial-mesenchymal transition and metastasis by controlling TIF1γ in non-small cell lung cancer. *Mol Cancer* 2018, 17: 140–148
39. Eser PÖ, Jänne PA. TGFβ pathway inhibition in the treatment of non-small cell lung cancer. *Pharmacol Ther* 2018, 184: 112–130